ELSEVIER

On the thermal behavior of Li bis(oxalato)borate LiBOB

Ella Zinigrad, Liraz Larush-Asraf, Gregory Salitra, Milon Sprecher, Doron Aurbach[*]

Bar-Ilan University, Ramat-Gan 52900, Israel

Abstract

The lithium salt, bis(oxalato)borate, $LiBC_4O_8$ (LiBOB), is one of the most important Li salts which are explored today in connection with R & D of novel, high energy density rechargeable Li batteries. The thermal stability of this salt in the temperature range of 40–350 °C was rigorously studied by accelerating rate calorimetry (ARC), differential scanning calorimetry (DSC), and thermal gravimetric analysis (TGA). XRD, FTIR, SEM, and ICP were used to analyze the products of its thermal decomposition reactions. Studies by DSC and pressure measurements during ARC experiments with LiBOB detected an endothermic reaction with an onset at ~293 °C, involving a complete irreversible decomposition of the LiBOB in which gaseous products are formed. In the first stage, $Li_2C_2O_4$ (crystalline), B_2O_3 (glass), CO and CO_2 gases are formed in both confined and open volumes. The next (final) stage in the thermal reactions is an irreversible formation of lithium triborate LiB_3O_5 (glass).
© 2007 Elsevier B.V. All rights reserved.

Keywords: ARC; DSC; TGA; Thermal decomposition; LiBOB

1. Introduction

The new lithium salt, bis(oxalato)borate, was recently proposed by Lischka et al. [1] and Xu and Angell [2] as a very promising and advantageous electrolyte for rechargeable Li ion batteries, instead of the problematic $LiPF_6$, which is the commonly used Li salt in electrolyte solutions for commercial Li ion batteries.

During the last ten years, a number of papers appeared in the literature demonstrating the good performance of graphite anodes and transition metal cathodes in solutions containing LiBOB (compared to their behavior in solutions based on $LiPF_6$). It was also demonstrated that the thermal stability of electrolyte solutions for Li ion batteries based on LiBOB is much higher than those based on other Li salts (e.g., $LiPF_6$, $LiBF_4$) [3]. Hence, it is clear that the intrinsic thermal behavior of LiBOB is interesting and important regards with R & D of novel and safer Li ion batteries. Indeed, in recent years some reports on the thermal studies of LiBOB appeared in the literature, as summarized below. According to thermogravimetric experiments, lithium-bis(oxalato)borate is fully stable up to approximately 300 °C [1]. Differential thermal analysis combined with thermogravimet-

ric analysis (DTA–TGA), using a scanning rate of 10 °C min^{-1}, showed that LiBOB is stable up to 302 °C. Beyond this temperature, it decomposes, rather than melts [2]. This salt is chemically stable in organic solutions, but is reported to slowly decompose by hydrolysis to $LiBO_2$ and LiOOCCOOH [2]. Amine et al. [4] presented the thermogravimetric curve for LiBOB in the temperature range of 20–600 °C. Yu et al. [5] reported on the stability of LiBOB in the temperature range of 240–300 °C, and on LiBOB decomposition to Li_2CO_3, B_2O_3, CO_2, and CO when the temperature is higher than 300 °C. They observed a weight loss related to two processes at temperatures in the region of 320 °C and 450 °C. It was reported that the decomposition of LiBOB at 302 °C produces B_2O_3 and CO_2 [6].

Yet despite past studies of LiBOB and its solutions regards both electrochemical performance and thermal behavior, there is still not a comprehensive picture of the intrinsic thermal behavior of this salt nor a clear determination of all the products of its thermal reactions. The aim of the present work is to remedy said differences, and achieve a comprehensive understanding of the calorimetric response of LiBOB and a rigorous analysis of its decomposition products.

2. Experimental

Highly purified LiBOB salt was obtained from Chemetall Inc. and was used as received. The pristine salt and its thermal

[*] Corresponding author. Tel.: +972 3 5318309; fax: +972 3 5351250.
E-mail address: aurbach@mail.biu.ac.il (D. Aurbach).

dissociation products were characterized by Fourier transform infrared (FTIR) spectroscopy (Magna 860 Spectrometer from Nicolet Inc., placed in a glove box under H_2O- and CO_2-free atmosphere), elemental analysis by an inductively coupled plasma (ICP) spectrometer (Ultima 2, Jobon Yvon Horiba), optical microscopy (AX70/AX70A, Olympus Inc.), scanning electron microscopy (SEM) (JEOL JSM 840), and X-ray diffraction using a D8 Advance System from Brucker Inc. XRD patterns were obtained using Cu K_α radiation ($\lambda = 1.54$ Å) at 40 mA and 40 kV. We used a cell which enabled the isolation of the sensitive samples from atmospheric gases by a polyester Mylar-type film, 90 μm thick, transparent to X-ray radiation. An accelerating rate calorimeter (ARC) from Arthur D Little Inc., Model 2000, a differential scanning calorimeter (DSC) from Mettler Toledo Inc., Model DSC 822, and thermogravimetry (TG, DTA) (SDT 2960, TA instrument) were used for the thermal analysis of LiBOB.

In the ARC measurements, about 1 g of salt was loaded in a titanium flask (8.2 ml volume) in an argon-filled glove box (VAC Inc.) and transferred to the ARC under purified Ar atmosphere. In the search for self-heating, the salt was heated from 40 to 300 °C in 5 °C increments at the rate of 2 °C min^{-1} at a sensitivity threshold of 0.02 °C min^{-1}. The controller was programmed to wait 15 min for the sample and the calorimeter temperatures to equilibrate, and then to search during 20 min for a temperature increase of 0.02 °C min^{-1}. After the ARC experiments, the titanium reaction vessel were cooled with liquid nitrogen until the pressure was close to the atmospheric pressure. The gaseous products were released through a specially designed high-pressure valve.

TGA–DTA measurements were conducted under pure nitrogen atmosphere in alumina crucibles, 70 μl in volume. DSC measurements in a confined volume were conducted in hermetically sealed, gold-plated stainless steel crucibles, 30 μl in volume (Mettler Toledo Inc.) over a temperature range of 40–350 °C. The crucibles were filled with about 10 mg of the salt, and then sealed in a glove box under argon atmosphere. The heating/cooling rate was 1 °C min^{-1}.

3. Results

Fig. 1 shows temperature and pressure changes (with time) measured during ARC experiments on 1.0 g of LiBOB heated up to 300 °C. There is no evidence of an exotherm in this temperature range. The significant pressure increase with an onset of 265 °C (Fig. 1a) and the negative slope in the temperature steps appearing at about 268 °C (Fig. 1b), may be explained by an endothermic decomposition of LiBOB. The gaseous products of this reaction were collected and analyzed (see below).

Fig. 2 presents TGA and DTA curves for LiBOB and Li oxalate samples. DTA curve b of LiBOB, shows two endothermic peaks at about 100 °C and 310 °C, respectively, accompanied by weight loss (TGA curve a). The first endotherm is attributed to the loss of adsorbed water, which amounts to ~0.06% of the sample as calculated from the TGA results. The second endotherm with an onset at about 293 °C (Fig. 2) is
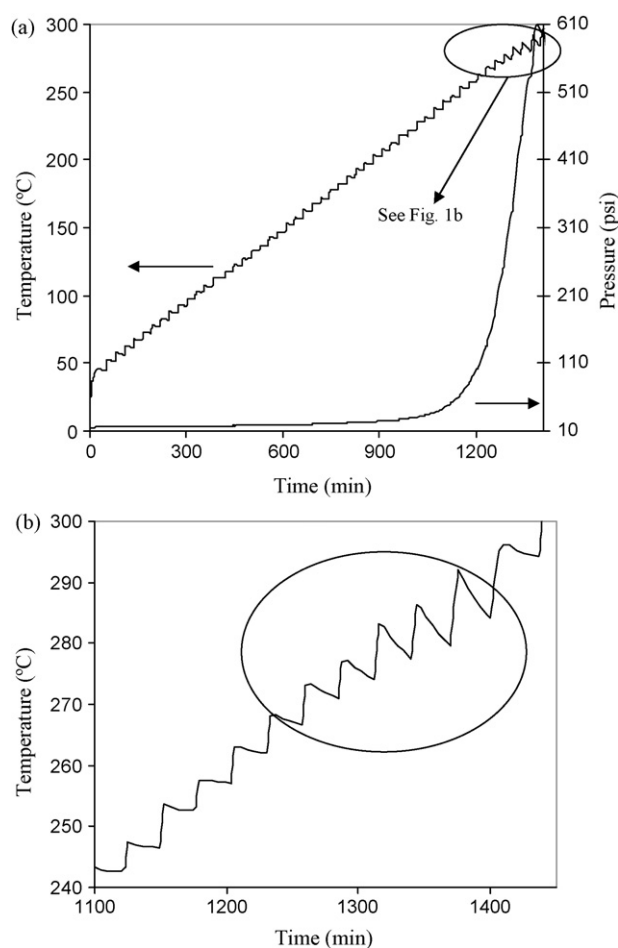

Fig. 1. (a) A typical ARC response during heating LiBOB. (b) The chart emphasizes the behavior in the temperature range 240–300 °C.

related to LiBOB decomposition. The weight loss calculated from the TGA and ARC measurements for the complete process is $61.2 \pm 0.5\%$.

Fig. 3 shows typical DSC heating curves obtained for LiBOB (a) and mixtures of Li oxalate–B_2O_3, 1:3 mol/mol (b) in closed crucibles. One endothermic process is to be seen in the temperature range 210–390 °C (Fig. 3a). It is identified as LiBOB
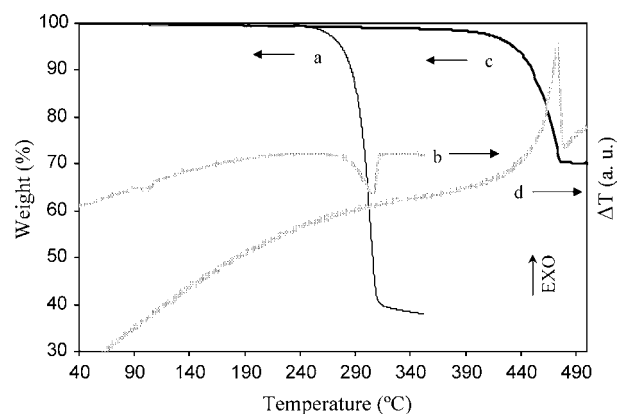

Fig. 2. TGA (a and c) and DTA (b and d) curves obtained by heating LiBOB samples at a rate of 1 °C min^{-1} (14.830 mg) (a and b), and Li oxalate (5.255 mg) (c and d).

Table 1
Parameters related to LiBOB decomposition, appearing in the DSC curves at a heating rate of $1\,°C\,min^{-1}$

| No.	Weight (mg)	(μmol)	Temperature interval (°C)	Onset temperature (°C)	Peak temperature (°C)	ΔU_r of decomposition (kJ mol^{-1})
1	3.587	18.49	280.4–328.7	297.04	309.80	41.10
2[*]	4.379	22.57	261.5–331.4	286.07	304.50	45.98
3	4.987	25.71	283.0–340.0	296.00	322.89	33.42
4	5.095	26.26	266.0–344.0	290.00	314.77	33.58
5	6.842	35.27	260.2–335.1	298.24	315.32	38.71
6	8.037	41.43	258.8–336.4	295.06	315.54	37.80
7	10.195	52.55	268.5–344.5	290.93	313.76	37.31
Average				293.33 ± 3.72	313.80 ± 3.81	38.27 ± 3.14

[*] An open crucible.
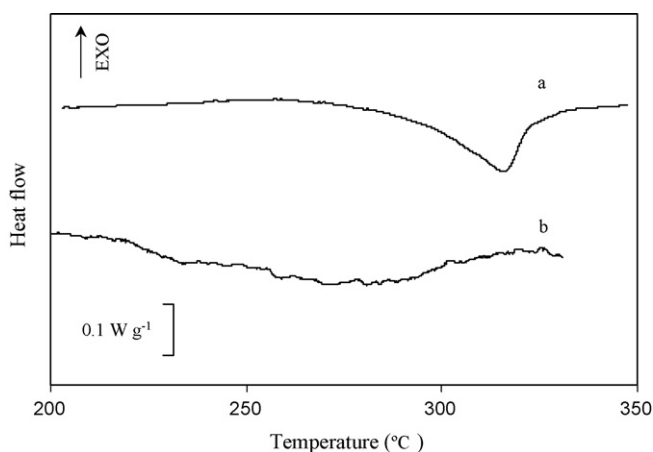
Fig. 3. DSC curves obtained by heating: (a) LiBOB sample, 8.037 mg; and (b) mixture Li$_2$C$_2$O$_4$–B$_2$O$_3$, 1:3 mol/mol, 1.717 mg. Heating rate $1\,°C\,min^{-1}$.

irreversible decomposition since DSC cooling curves did not show any peaks. The results of 7 different DSC tests at a heating rate of $1\,°C\,min^{-1}$ are summarized in Table 1. The onset of the endothermic dissociation of LiBOB is at about 293 °C. The decomposition heat is about 38 kJ mol^{-1} (196 J g^{-1}).

Fig. 3b showing the thermal behavior of a Li oxalate–B$_2$O$_3$ mixture, 1:3 mol/mol reflects an endothermic reaction between these two species in the temperature range that overlaps the range of LiBOB decomposition, with a reaction heat around 67.9 kJ mol^{-1} of reacting LiB$_3$O$_5$. This datum is very important for the discussion below.

Figs. 4 and 5 show SEM and optical micrographs respectively of pristine and heated LiBOB powder. The pristine white powder consists of elongated round particles with a length of 0.1–0.5 mm and a diameter of 0.05–0.25 mm. Surprisingly, the particles' shape and size did not change noticeably after heating to 350 °C (Fig. 4a and b) in spite of the weight loss of about 60%. They are non transparent under transmitted light (Fig. 5a) and do not demonstrate non homogeneity under polarized light (Fig. 5b).

Fig. 6 shows XRD patterns of the pristine salt and the solid decomposition product (collected after heating). The XRD patterns of the pristine LiBOB correlates well with literature data [7]. No observation of pristine LiBOB peaks after heating to 350 °C indicates a complete LiBOB decomposition. These powders, after heating in a closed volume in an ARC bomb, in DSC crucibles, and in opened alumina crucibles in TGA tests, show
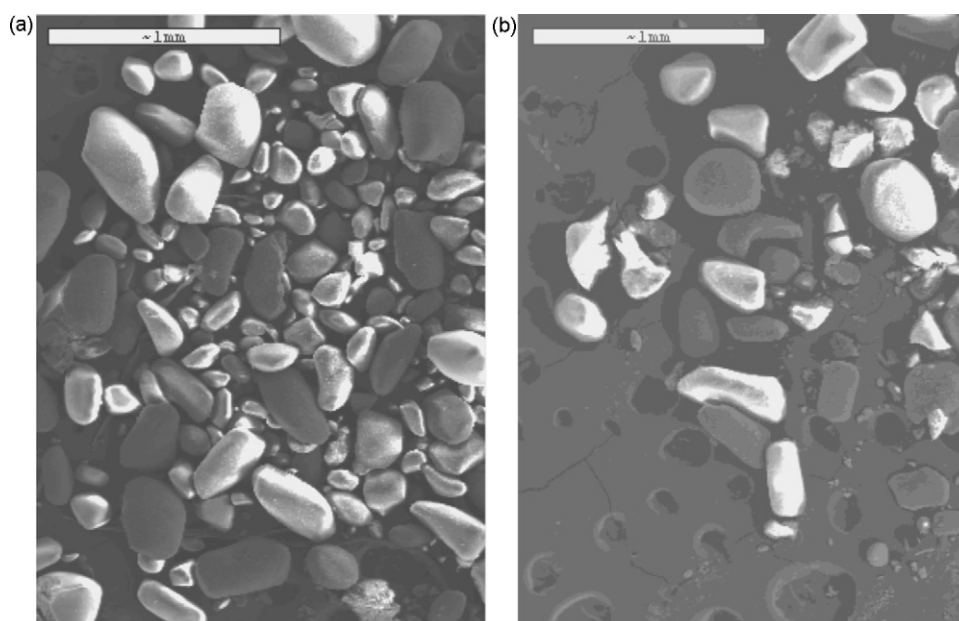

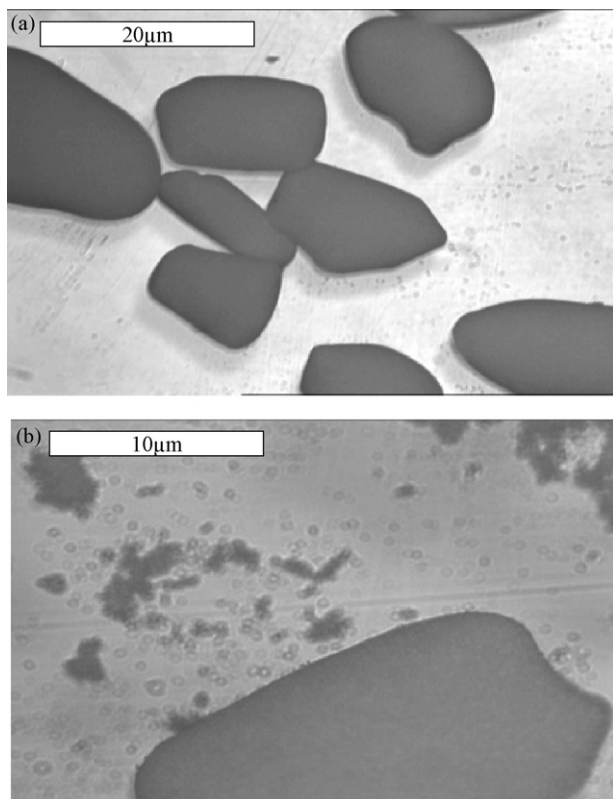Fig. 4. SEM micrographs of: (a) pristine LiBOB samples; (b) LiBOB after heating to 350 °C. A scale appears in each micrograph.

Fig. 5. Photomicrographs from optical microscope of the powder obtained after heating of LiBOB samples to 350 °C: (a) transmission (×5); (b) polarized light (×10).
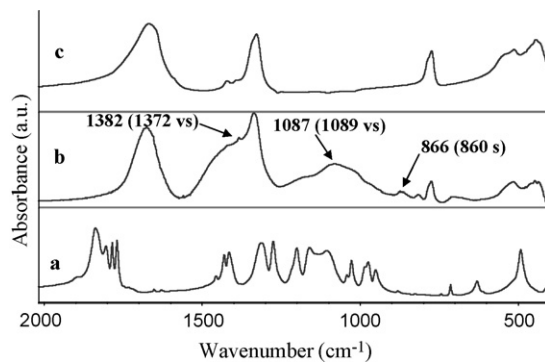

Fig. 7. FTIR spectra of: (a) pristine LiBOB powder [9]; (b) the powder obtained by heating LiBOB to 350 °C; and (c) Li oxalate powder is shown for comparison. The spectra were obtained by KBr pellet method.

identical XRD patterns. All peaks correspond to monoclinic lithium oxalate [8]. Storing of this product for 10 days at 300 °C did not cause any structural changes (confirmed by XRD and FTIR).

There is good agreement between the XRD measurements and the FTIR spectra (Fig. 7). As seen in Fig. 7, the IR bands of pristine LiBOB are not detected after heating to 350 °C, but all the expected IR peaks of Li oxalate can be seen in the spectrum of the thermal product.

Fig. 8 compares FTIR spectrum of the gaseous product of LiBOB thermal decomposition to the spectra of CO_2 and CO. From these studies, it is clear that the gaseous product of LiBOB decomposition comprises both CO_2 and CO. The discrepancy between FTIR signals of these gases occurs due to the fact that the absorbent coefficient of CO is near 7 times smaller than
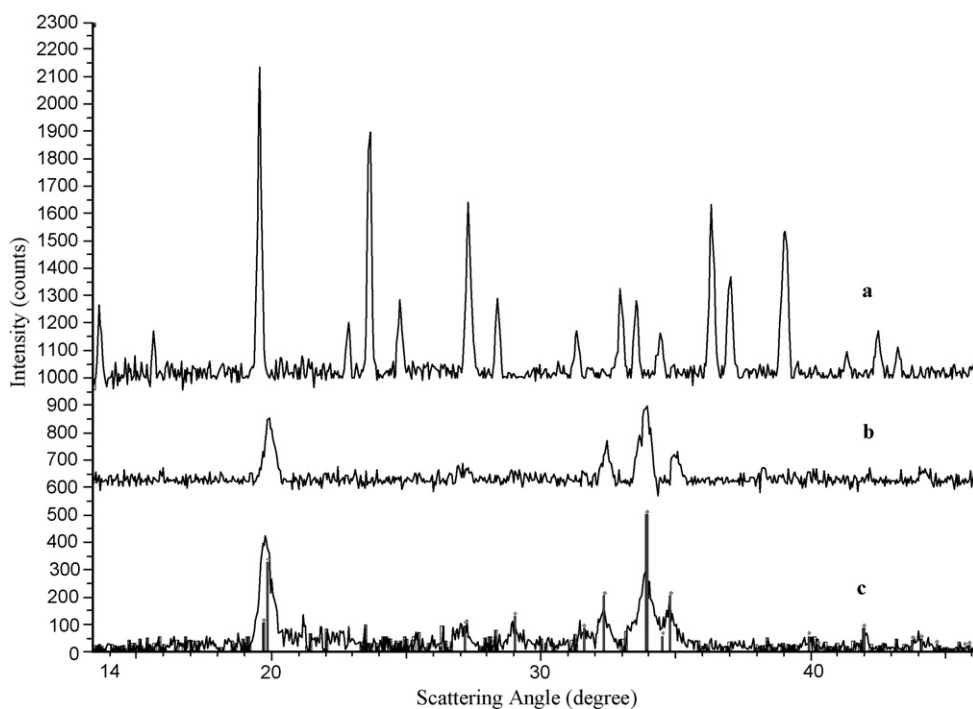

Fig. 6. XRD patterns of: (a) a pristine LiBOB powder; (b) a powder obtained by heating LiBOB to 350 °C; (c) same as (b) after storage at 300 °C for 10 days. Line marks of Li oxalate are shown for comparison.
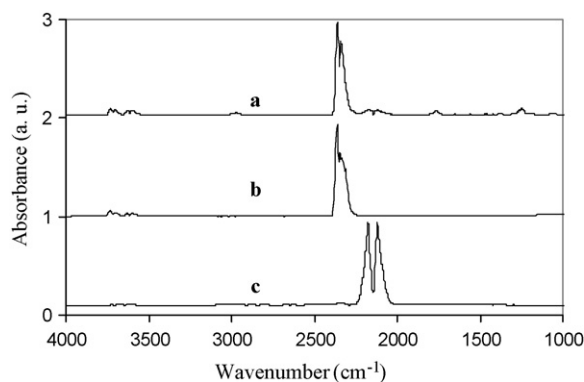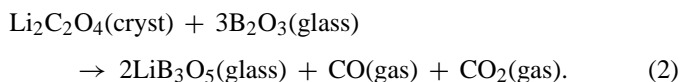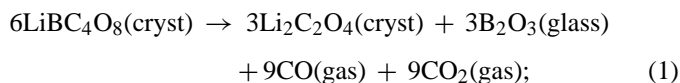
Fig. 8. FTIR spectrum of a gas phase that is formed in the ARC calorimetric bomb due to a thermal decomposition of LiBOB (a). Spectra of CO_2 (b) and CO (c) are presented for comparison.
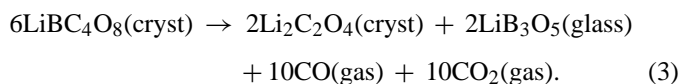
that of CO_2 at room temperature [10]. The solid product of LiBOB thermal decomposition was dissolved in distilled water and analyzed by ICP and found to contain 9.3% Li and 13.9% B.

4. Discussion

Based on the above results and as detailed below, it is suggested that the decomposition of LiBOB at ~300 °C occurs as follows:

$$6LiBC_4O_8(cryst) \rightarrow 3Li_2C_2O_4(cryst) + 3B_2O_3(glass)$$
$$+ 9CO(gas) + 9CO_2(gas); \qquad (1)$$

$$Li_2C_2O_4(cryst) + 3B_2O_3(glass)$$
$$\rightarrow 2LiB_3O_5(glass) + CO(gas) + CO_2(gas). \qquad (2)$$

The overall thermal decomposition process of LiBOB is:

$$6LiBC_4O_8(cryst) \rightarrow 2Li_2C_2O_4(cryst) + 2LiB_3O_5(glass)$$
$$+ 10CO(gas) + 10CO_2(gas). \qquad (3)$$

The calculated weight loss for decomposition of LiBOB according to Eq. (1) is 55.7%. However, the TGA and ARC experiments show a greater weight loss upon thermal decomposition. The TGA data (Fig. 2) show a weight loss of about 62%. Clearly, an additional reaction involving gas evolution is taking place. This cannot be the decomposition of lithium oxalate to carbonate, because to our TGA–DTA findings (Fig. 2) as well as literature data [12] this occurs only above 400 °C. Furthermore, FTIR spectra of the LiBOB samples after heating to 350 °C indicated the absence of B_2O_3 as a final decomposition product (Fig. 7). The IR spectrum of the vitreous B_2O_3 contains a stronger absorption band at ~1265 cm^{-1}, a weak absorption band at ~720 cm^{-1}, and also a shoulder situated at ~1400 cm^{-1} [11].

Hence, we suggest reaction (2) above as a follow up process that well explains both the weight loss observed and the absence of B_2O_3 in the end product.
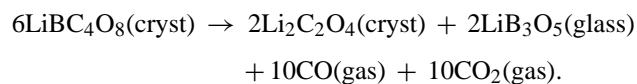
All the B_2O_3 produced by the first step (Eq. (1)) is consumed in the second (Eq. (2)). However, this second reaction consumes only 1/3 of the Li oxalate formed in the first. This correlates well with the fact that the final products of LiBOB decomposition contain Li oxalate, as evidenced by both XRD and FTIR (Figs. 6 and 7). The calculated weight loss for decomposition equation (3) is 61.6%. This matches the experimental result (DTA–TGA, Fig. 2) of ca. 62%. The Li triborate (LiB_3O_5) is formed as a non crystalline glass phase and cannot therefore be identified by X-ray diffraction. However, Fig. 7 presents FTIR spectra of pristine LiBOB, of a sample after heating to 350 °C, and of Li oxalate for comparison. The spectrum of the decomposed sample clearly shows oxalate bands at 449, 516, 775, 1330, and 1665 cm^{-1}, and three new bands at 1087, 1382 and 866 cm^{-1} (not related to oxalate). These peaks can be assigned to the strong bands of LiB_3O_5 at 1372, 1087 and 860 cm^{-1} [13]. The ICP analysis of the solid product after heating LiBOB to 350 °C showed the presence of 9.3% Li and 13.9% B. This fits well the composition expected for solid product suggested by Eq. (3), namely a mixture of $Li_2C_2O_4 + LiB_3O_5$ (9.4% Li and 14.5% B).

The following experiment was carried out to confirm the occurrence of the reaction postulated in Eq. (2). Mixtures containing $Li_2C_2O_4:B_2O_3$ 1:3 mol/mol were thoroughly ground in an agate mortar and pestle and were then subjected to DSC in closed crucibles up to 500 °C. A pronounced broad endothermic peak appears in the temperature range that overlaps the range in which LiBOB decomposes (Fig. 3). The onset of this peak is near 210 °C that is ca. 80 °C lower than the onset of the LiBOB decomposition peak (Eq. (1)). This temperature is far for the oxalate decomposition (above 400 °C) and the endotherm is attributed only to reaction (2). Hence, reaction (2) begins immediately upon the formation of $Li_2C_2O_4$ and B_2O_3 by LiBOB decomposition (Eq. (1)). The heat of the endothermic reaction between Li oxalate and B_2O_3 was found to be about 67.9 kJ mol^{-1} of the product LiB_3O_5. According to Eq. (3), only 1/3 mol of LiB_3O_5 is formed by the decomposition of 1 mol of LiBOB. Therefore, about $67.9/3 \approx 22.6$ kJ mol^{-1} of LiBOB decomposed is absorbed for the formation of 1/3 mol of LiB_3O_5. This value is part of the overall heat of decomposition LiBOB, of namely about 38 kJ mol^{-1} (see Table 1). Consequently, the heat of the first decomposition step of LiBOB, Eq. (1), is near $38 - 23 = 15$ kJ mol^{-1}. XRD measurements of the product of heating the $Li_2C_2O_4$–B_2O_3 mixture (up to 350 °C) showed no evidence of a crystalline phase.
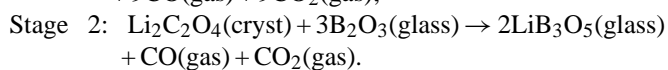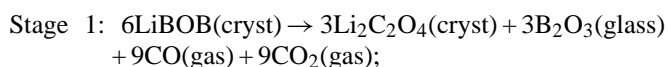
A mixture Li_2O–B_2O_3 containing 75 mol% B_2O_3 should undergo slow crystallization upon storage at elevated temperatures, above 500 °C [14]. The crystals of LiB_3O_5 were grown on a seed from the solution-melt using the method of temperature lowering [15]. The end product of LiBOB decomposition was stored at 300 °C during 10 days by further cooling at a rate of 1 °C min^{-1}, followed by XRD measurements. (This is the highest temperature at which a mixture containing Li oxalate can be heated and remains stable). No evidence for the formation of any new crystalline phase, except the existing Li oxalate, was observed by X-ray diffraction (Fig. 6c).

5. Conclusions

The study of LiBOB decomposition by ARC, DSC and TGA at elevated temperatures, the analysis of the decomposition products by XRD, FTIR and element analysis (ICP), and further thermal studies of mixtures of Li oxalate and B_2O_3 showed that LiBOB decomposes in an irreversible endothermic reaction at an onset temperature of $293 \pm 4\,°C$ according to the following equation:

$$6LiBC_4O_8(cryst) \rightarrow 2Li_2C_2O_4(cryst) + 2LiB_3O_5(glass)$$
$$+ 10CO(gas) + 10CO_2(gas).$$

This reaction occurs in two stages in the same temperature range:

Stage 1: $6LiBOB(cryst) \rightarrow 3Li_2C_2O_4(cryst) + 3B_2O_3(glass) + 9CO(gas) + 9CO_2(gas)$;

Stage 2: $Li_2C_2O_4(cryst) + 3B_2O_3(glass) \rightarrow 2LiB_3O_5(glass) + CO(gas) + CO_2(gas)$.

References

[1] U. Lischka, U. Wietelmann, M. Wegner, German Pat. DE 19829030 C1 1999.

[2] W. Xu, C.A. Angel, Electrochem. Solid-State Lett. 4 (2001) E1–E4.

[3] C.K. Xu, S.S. Zhang, T.R. Jow, W. Xu, C.A.L. Angel, Electrochem. Solid-State Lett. 5 (2002) A26–A29.

[4] K. Amine, J. Liu, S. Kang, I. Belharouak, Y. Hyung, D. Vissers, G. Heriksen, J. Power Sources 129 (2004) 14–19.

[5] B.-T. Yu, W.-H. Qui, F.-S. Li, G.-X. Xu, Electrochem. Solid-State Lett. 9 (2006) A1–A4.

[6] K. Xu, S. Zhang, T.R. Jow, W. Xu, C.A. Angel, Electrochem. Solid-State Lett. 5 (2002) A26–A29.

[7] P.Y. Zavalij, S. Yang, M.S. Whittingham, Acta Cryst. B59 (2003) 753–759.

[8] JCPDS-ICDD, 00-024-0646.

[9] L. Larush-Asraf, M. Biton, H. Teller, E. Zinigrad, D. Aurbach, J. Power Sources, in press.

[10] K. Wakatsuki, S.P. Fuss, A. Hamins, M.R. Nyden, Proceedings of the Combustion Institute 30, 2005, pp. 1565–1573.

[11] M.M. Girgis, A.M. Elawad, Thermochim. Acta 214 (1993) 291–303.

[12] I. Ardelean, M. Toderas, P. Pascuta, Modern Phys. Lett. B 17 (2003) 1175–1179.

[13] U. Moryc, W.S. Ptak, J. Mol. Struct. 511–512 (1999) 241–249.

[14] B.S.R. Sastry, F.A. Hummel, J. Am. Ceram. Soc. 41 (1958) 7–17.

[15] Yu.F. Shepelev, R.S. Bubnova, S.K. Filatov, N.A. Sennova, N.A. Pilneva, J. Solid State Chem. 178 (2005) 2987–2997.